First-principles investigation of structural and electronic properties of ultrathin Bi films

Yu. M. Koroteev,[1] G. Bihlmayer,[2] E. V. Chulkov,[3,4] and S. Blügel[2]
[1]*Institute of Strength Physics and Materials Science, RAS, 634021 Tomsk, Russia*
[2]*Institut für Festkörperforschung, Forschungszentrum Jülich, D-52425 Jülich, Germany*
[3]*Departamento de Física de Materiales, UPV/EHU and Centro Mixto CSIC-UPV/EHU, Apartado 1072, 20080 San Sebastiàn/Donostia, Spain*
[4]*Donostia International Physics Center (DIPC), 20018 San Sebastiàn/Donostia, Spain*
(Received 9 November 2007; revised manuscript received 21 December 2007; published 28 January 2008)

Employing first-principles calculations, we perform a systematic study of the electronic properties of thin (one to six bilayers) films of the semimetal bismuth in (111) and (110) orientation. Due to the different coordination of the surface atoms in these two cases, we find a large variation of the conducting properties of the films, ranging from small-band-gap semiconducting to semimetallic and metallic. The evolution of the Bi(111) and Bi(110) surface states can be monitored as a function of the film thickness. Another interesting feature is provided by the strong spin-orbit effects in Bi and the resulting Rashba-type spin splitting of the surface states. The relaxations, band structures, Fermi surfaces, and densities of states are presented and discussed with respect to possible applications in the field of spintronics.

DOI: 10.1103/PhysRevB.77.045428 PACS number(s): 73.20.−r, 71.18.+y, 71.70.Ej

I. INTRODUCTION

The electronic properties of ultrathin films of semimetals have attracted considerable interest in the last few years: Due to the unique electronic structure—ideally, the Fermi surface reduces to a single point—unconventional transport properties can be anticipated. For example, the graphene sheet is regarded as a model system that offers the possibility to study the "massless Dirac particle" in an experimentally rather easily accessible system.[1] Interesting physical properties, such as magnetic edge states or the spin Hall effect, have been predicted for stripes of graphene,[2] as well as for another semimetal, bismuth.[3] Experimentally, ultrathin films of Bi on semiconducting substrates can be realized,[4] showing interesting effects in the electronic structure.[5] The surfaces of Bi are characterized by prominent surface states which dominate the density of states around the Fermi level. The transport properties can, therefore, be considered to originate only from these states, forming a two-dimensional (2D) electron gas localized at the surface of the semimetal. The strong spin-orbit coupling in Bi furthermore leads to a strong spin splitting of the surface states,[7] which was experimentally observed on a Bi(110) surface[8] and in thin Bi(111) films.[9] Note that we use rhombohedral indexing to specify the Bi surfaces.

While graphene is formed from electronically rather independent 2D entities with a honeycomb lattice structure, which are connected via weak dispersion forces, in bismuth, different scenarios arise. The Bi(111) surface is characterized by hexagonal closed packed layers, which are organized in the form of bilayers, with the nearest-neighbor bonds forming a buckled honeycomb lattice (left of Fig. 1). The surface states are mainly localized in the topmost bilayer. Structurally, bilayers in Bi form a stable unit with strong intrabilayer bonds, while the interbilayer bonding is much weaker.[10,11] The Bi(110) surface is also organized in bilayers, forming an almost flat sheet (Fig. 1, right) with the atom of the second layer placed near the center of the quasisquare lattice of the first layer.[12] The electronic character of the surface states arising on this surface differs from the (111) surface since one nearest neighbor bond of Bi is broken, leaving a dangling bond. Therefore, the Bi(110) surface state is quite different from the Bi(111) surface state, forming a surface state band throughout the 2D Brillouin zone.[8] A similar behavior of the surface state is observed on the quasihexagonal Bi(100) surface. Here, no localization of the states in bilayers is observed and the surface states extend considerably into the volume of the crystal.[13]

Experimentally, thin Bi(111) films [in short hexagonal notation, this corresponds to Bi(001)] with a thickness down to seven bilayers have been prepared on a Si(111) substrate.[4] Below this thickness, a structural transformation to a A17 allotrope crystal structure occurs, forming a quasisquare surface unit cell, such as the Bi(110) surface, but with strong corrugation. For the seven bilayer film, surface states and

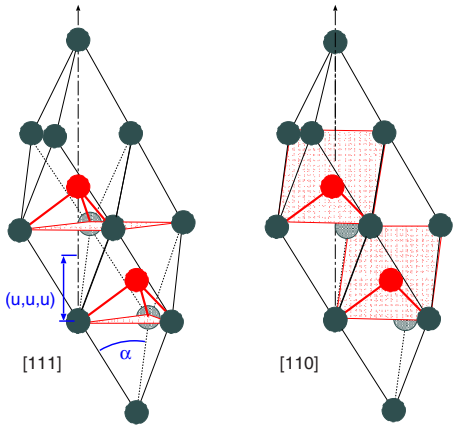

FIG. 1. (Color online) Bulk structure of Bi with indication of the (111) planes (shaded red, left) and the pseudosquare (110) planes (shaded red, right). The nearest neighbor bonds are indicated with thick (colored) lines. The colored and black atoms connected by these bonds form stable bilayer units.

quantum well states are formed and a Fermi surface arises, which is already very similar to what is observed on semi-infinite Bi(111) crystals.[5,14] For thinner films, which might be obtained using different substrates and/or growth conditions, the situation can be quite different, leading to semiconducting or semimetallic films.

In this work, employing calculations based on density functional theory (DFT), we investigate the structural properties and the electronic structure of thin films of Bi(111) and Bi(110), ranging from a single bilayer up to six bilayers. Our focus is on the electronic states near the Fermi level, which, depending on the orientation and film thickness, can give rise to semiconducting, metallic, or semimetallic behavior. Comparing these results to what has been obtained for thicker films,[7] the evolution of the surface states can be analyzed. Since the electronic structure of thin films is almost not influenced by the presence of a weakly interacting substrate on which these films might be grown, these data can serve as a basis for the tailoring of thin films or nanostructures with specific electronic properties.

II. METHOD OF CALCULATION

For our calculations, we employed the local density approximation to DFT in the form given by Moruzzi *et al.*[15] We use the full potential linearized augmented plane wave method[16] in thin film geometry as implemented in the FLEUR code.[17] Spin-orbit coupling (SOC) was included in the self-consistent calculations as described by Li *et al.*[18] The size of the muffin-tin spheres of the Bi atoms was chosen to equal 2.5 a.u.; the cutoff for the basis functions was 3.6 a.u.$^{-1}$. For the self-consistent calculations of the (111) surfaces, the irreducible part of the two-dimensional Brillouin zone (I2BZ) was sampled at 21 **k** points; for the (110) surface, 36 **k** points were used. For the generation of the densities of states (DOSs) and the Fermi surfaces, 121 and 225 **k** points in the I2BZ were employed for the (111) and the (110) surfaces, respectively. The relaxations of the first two layers of the films were performed including spin-orbit coupling in the calculations. For the calculation of the "semi-infinite" Bi(111) surface, we used a 22 layer Bi film that was terminated on one side by hydrogen to eliminate the surface states.

III. RESULTS

Bulk Bi crystallizes in a rhombohedral Bravais lattice with a rhombohedral angle α of about 57.3° and two atoms in the unit cell, located at positions $\pm(u,u,u)$, where $u=0.234\,07$ at 4.2 K (Ref. 19). If α were 60°, the lattice would be face-centered cubic, with two atoms in the unit cell; if additionally $u=1/4$, the lattice would be simple cubic (sc) with one atom in the unit cell. Starting from this sc unit cell, the layers of the Bi(111) films can be imagined as sc (111) layers, i.e., they have hexagonal closed packed structure and are ordered in an *ABCABC* stacking sequence along the surface normal. Since u deviates from the value of 1/4, two different interlayer distances arise, which alternate along the stacking sequence. The long and the short (111) interlayer distances differ by $(4a_{sc}/\sqrt{3})(1-4u)$, if a_{sc} is the lattice constant of the imagined simple cubic unit cell. Two layers separated by a short interlayer spacing are connected by three nearest-neighbor bonds, forming the stable bilayers described in the Introduction. The fact that the rhombohedral angle α is smaller than 60° just leads to an uniform expansion of the interlayer distances. The resulting structure is sketched on the left of Fig. 1.

Likewise, the layers of a Bi(110) film or surface can be imagined to originate from the (100) planes of a simple cubic lattice. To accommodate for a value of u different from 1/4, a $c(2\times2)$ unit cell has to be chosen, and the two atoms in this unit cell are slightly displaced along a sc (111) direction in opposite ways. This gives rise to a small buckling of the sc (100) planes and the middle atom is shifted slightly away from the center, toward one side of the $c(2\times2)$ unit cell. This leaves only one mirror plane in the cell. The nonideal angle α causes a small rectangular deformation of this unit cell, where the longer side is parallel to the mirror plane. This results in almost flat, pseudosquare layers, as illustrated on the right of Fig. 1. Since there are only two nearest-neighbor bonds in these layers, perpendicular to the surface plane, a dangling bond is formed.

A. Bi(111)

Bulk Bi is a semimetal, with a small hole pocket at the T point and an electron pocket at the L point.[20] Projected onto the (111) surface, the T point is located at the two-dimensional zone center ($\bar{\Gamma}$), while the L points fall at the zone edges, forming the $\bar{M}$ points. The electron and hole pockets are very shallow, extending just 27 and 11 meV, respectively, beyond the Fermi level. In first-principles calculations, these values are typically overestimated and depend quite sensitively on the internal parameter u, which is overestimated in the calculations.[21] Therefore, it is possible that in the band structures of thin films, which are obtained using the calculated relaxations, the states around the $\bar{\Gamma}$ points appear at somewhat too high energies.

1. Structural properties

As can be seen from Fig. 1 (left), in Bi(111) films, one can identify bilayers connected by nearest-neighbor bonds. Therefore, like in bulk, also on a (111) surface, each Bi atom can form three nearest-neighbor bonds, if the topmost bilayer is not broken.

The relaxations of the Bi(111) films are summarized in Table I. We relaxed the first two interlayer distances, d_{12} and d_{23}, keeping the rest of the structure in the ideal, bulklike geometry as obtained from a bulk calculation. Since the nearest-neighbor bonds connect two layers with a small interlayer distance, we assumed that d_{12} is smaller than d_{23}, an observation that was also found experimentally for a Bi(111) surface of a semi-infinite crystal.[10] From the relaxations in Table I, it can be seen that indeed the relaxations Δd_{12} are very small, supporting the idea that stable Bi(111) bilayers are formed. In contrast, the relaxations between the second and third layers are quite substantial, indicating a weak interbilayer bonding. The values for the interlayer distances are

TABLE I. Structural parameters of Bi(111) films with one to six bilayer (BL) thickness: the changes of the interlayer distance $\Delta d_{i,j}$ of the layers i and j ($i=1$ is the surface layer) are given with respect to the calculated ideal interlayer distance of the bulk structure, $d_{i,i+1}=1.667$ and 2.288 Å for odd and even i, respectively.

Distance	One BL	Two BL	Three BL	Four BL	Five BL	Six BL
Δd_{12} (%)	0.0	−1.0	−0.8	0.0	0.7	0.9
Δd_{23} (%)		6.2	7.8	6.1	6.6	6.5

converging quickly with the film thickness, e.g., for a seven bilayer film, relaxations of 0.6% and 6.2% were found for Δd_{12} and Δd_{23}, respectively.[10] From the calculations of thicker films without SOC, we know that the next interlayer distance Δd_{34} is a small contraction in the order of magnitude of Δd_{12}, while Δd_{45} is a bit larger again, amounting to about one third the value of Δd_{23}.[10] This periodic pattern of small contractions and expansions is also found for the three to six BL films, decaying quickly to $\Delta d_{67}=0.2\%$ in the thickest film.

2. Electronic properties

We have concluded from the relaxations that Bi(111) bilayers form stable entities with strong nearest-neighbor bonds. This is also reflected in the electronic structure: In a single BL, the six Bi p states split into three bonding and three antibonding states forming a gap around the Fermi level (upper left graph of Fig. 2). As can be seen from the comparison between the band structures obtained from calculations without (blue) and with (red and/or black) spin-orbit coupling included, in this case, SOC decreases the gap but the semiconducting character is retained. This is quite opposite to the bulk, where a calculation without SOC yields metallic behavior and only inclusion of spin-orbit coupling leads to a semimetallic electronic structure.

In the case of a two bilayer Bi(111) film, the scalar relativistic calculation (i.e., without the inclusion of spin-orbit coupling) results in a metallic behavior and like in the bulk only SOC leads to semimetallic properties (upper right of Fig. 2). Without spin-orbit coupling, a band crosses the Fermi level near $\bar{\Gamma}$, a situation which is similar to the behavior of the surface state of a Bi(111) surface[7]: The (111) projected bulk band structure of Bi without SOC has a rather large gap around the Fermi level (E_F) at the zone center, where a surface state forms. Including SOC, the valence band reaches up to E_F, pushing the surface state up in energy (to smaller binding energies). In the case of the two BL Bi(111) film, we can already see the precursor of this surface state forming two bands, one above and one below the Fermi level. In contrast to the semi-infinite surface, where the Rashba-split surface state has degeneracies at the $\bar{\Gamma}$ and $\bar{M}$ points (cf., lower right of Fig. 2 and Ref. 7), here these degeneracies are removed by the strong interactions between the upper and the lower surface of the film (cf., Ref. 5). As the film thickness increases, we can see that these splittings decrease as can be expected from the increasing separation of the upper and lower surfaces. However, the screening in Bi is—as compared to metals—rather weak, and even 40 BL films still show a finite splitting at $\bar{M}$. Due to the almost linear dispersion of the underlying bulk band structure,[5] this splitting can be expected to decrease by a factor 2 if the number of layers is doubled in these films. Since the dispersion of the bulk bands along Γ-T is rather flat, the density of quantum well states is higher at the zone center than at $\bar{M}$, where the dispersion of the bulk bands is high. This causes the different localization lengths of the states near the $\bar{\Gamma}$ and $\bar{M}$ points and the stronger splitting of the bands at the zone boundary. The splitting of the two bands around E_F decreases faster near the $\bar{\Gamma}$ point; nevertheless, the two BL and three BL films remain semimetallic with the bands just touching

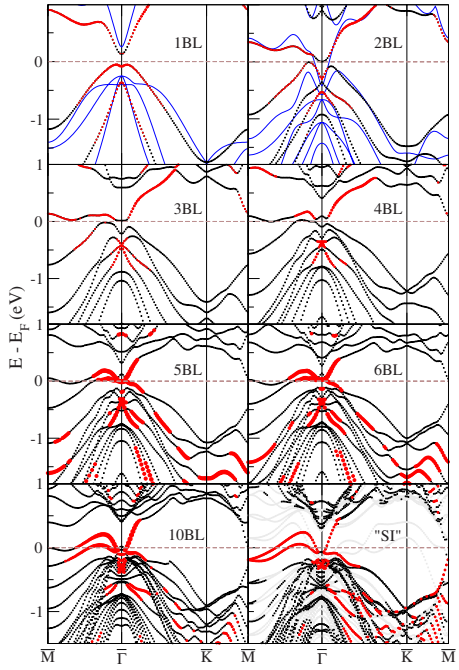

FIG. 2. (Color online) Band structures of Bi(111) films with one to six bilayer thickness as compared to a thicker (ten BL) film and a semi-infinite ("SI") crystal surface. In the figures for one to four bilayers, all states which have more than 10% of their weight in the vacuum are marked in red, and in the thicker films states located predominantly (more than 25%, 22%, 15%, and 5% for five, six, ten BL and the semi-infinite crystal surface, respectively) in the surface, BLs are marked by full (red) circles. The gray bands in the SI band structure are states from the lower, H-terminated part of the film. All band structures were obtained for the relaxed geometries. In the band structures for the one and two BL films, we include also the result obtained without spin-orbit coupling (thin blue lines): in all other results (dots and circles), SOC was included in the self-consistent calculations.

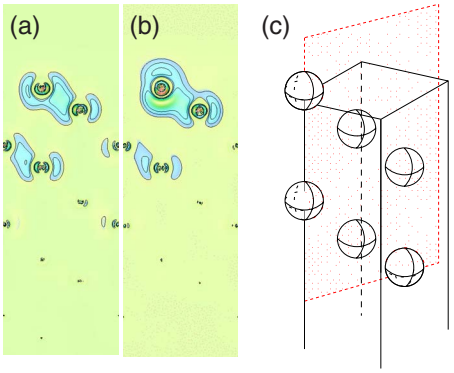

FIG. 3. (Color online) [(a) and (b)] Charge density contours for the surface states at a **k** point from the line $\overline{\Gamma M}$ near $\bar{\Gamma}$ for a Bi(111) surface (cf., lower right band structure in Fig. 2). (a) presents the lower branch of the surface state, while in (b), the charge density for the upper branch is shown. The geometry of the film and the plane, where the cut was taken, is sketched in (c).

the Fermi level. This is supported by DOS calculations.

Films thicker than four BL finally show surface states, which are already quite similar to the semi-infinite case. A comparison of the ten BL case to experimental results is given in Refs. 5 and 6. In Fig. 2, we marked the surface state character by analyzing the weight of the wave function in the surface bilayer, rather than in the vacuum. Since the Bi(111) surface state is a $p_{(x,y)}$-like surface state (which gains some p_z character by orbital mixing due to SOC), its weight in the vacuum is rather small. Charge density plots of two cases are shown in Fig. 3. The strongly localized surface states on Bi(111) clearly reflect the bilayer structure in this surface, while other surface orientations, such as the Bi(100) surface, show a delocalization of the surface states through several layers.[13] In contrast to the (100) surface, the (110) surface state remains rather localized at the surface, as will be shown below.

3. Fermi surfaces

From the band structures (Fig. 2), we see that thin Bi(111) films up to three bilayers have semiconducting or semimetallic properties. In the case of a four BL film, we observe that the bands around the Fermi level form small electron and hole pockets along the line $\overline{\Gamma M}$. As can be seen from Fig. 4, these pockets are quite narrow and stretched and increase slightly in size as we go from the four BL case to the five and six bilayer films. In the case of the six BL film, the hole pockets merge around the $\bar{\Gamma}$ point, forming a star, while experimentally already for nominally 6.8 BL films, the small hexagonal feature around the zone center was observed,[5] an electron pocket which is also found on the (111) surface of bulk Bi.[14] A detailed analysis of the calculation results shows that the precise position of the surface state bands around the $\bar{\Gamma}$ point depends quite sensitively on the projected bulk band structure in this region in **k** space. As we noted above, the hole pocket of bulk Bi is overestimated in the calculations and this is caused by an overestimation of the internal parameter u. For thicker films, we can correct for this deficiency and use the experimental value for u in the inner layers, which are not relaxed. Then, as can be seen in the case of the ten BL film (lower right of Fig. 4), the hexagonal pocket is nicely reproduced and the Fermi surface matches the experimental observation (note that the small hole pocket at $\bar{\Gamma}$ is a bulk feature, not observed in the experiments).

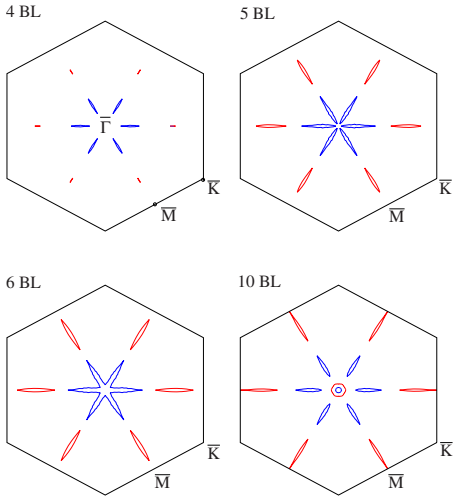

FIG. 4. (Color online) Fermi surfaces for Bi(111) films with four to six bilayer thickness and for a ten BL film. The electronic structure was obtained including spin-orbit coupling. Electron pockets are shown in red, while hole pockets are indicated by blue color.

Since, beyond a critical thickness, the Fermi surfaces of Bi(111) films are quite independent of the film thickness, these films would be an ideal playground for transport experiments. On a given side of the film, the states show a significant spin polarization due to the Rashba effect,[9] and this can give rise to spin-dependent phenomena, as was already observed for the Bi(110) surface.[8] The particular geometry of the Fermi surface, which has for very thin films no states in the $\overline{\Gamma K}$ direction, should also be observable in orientation-dependent transport measurements as could be performed with a four-tip scanning tunneling microscope.

B. Bi(110)

1. Structural properties

As discussed before, the Bi(110) surface shows a slightly buckled pseudosquare lattice with two atoms in the unit cell. It can be seen from the right part of Fig. 1 that in the A7 structure, this buckling moves two atoms which are stacked (almost) on top of each other either closer together or further apart. In the A17 allotrope, in contrast, vertically neighbored atoms are displaced in the same (vertical) direction and the corrugation is stronger.[4] In other words, in the A7 structure in two successive bilayers, the corrugation is such that the valleys are stacked on top of the hills (and vice versa), while in the A17 structure, valleys are stacked on valleys and hills on hills. On the (110) surface, the constraint of the bulk "substrate" counteracts this tendency to form puckered layers and the A7 structure is kept. In the following, we will only investigate "A7-type" relaxations to get a clear picture of the

TABLE II. Structural parameters of Bi(110) films with one to six bilayer (BL) thickness: the changes of the interlayer distance $\Delta d_{i,j}$ of the layers i and j ($i=1$ is the surface layer) are given with respect to the ideal interlayer distance of the bulk structure, $d_{i,i+1}=0.142$ and 3.087 Å for odd and even i, respectively. The in-plane displacements of the atoms within the bilayer i with respect to the bulk structure were found to be less than 0.01 Å.

Distance	One BL	Two BL	Three BL	Four BL	Five BL	Six BL
Δd_{12} (%)	318	−102	−127	−141	−75	−142
Δd_{23} (%)		0.3	1.4	0.5	0.4	0.4

evolution of the Bi(110) surface state from thinner films.

While a single Bi(110) bilayer shows a substantial increase of the corrugation, we can see from Table II that in thicker bilayer films, a tendency to flatten the outmost layer arises. A relaxation of −100% corresponds to a flat layer, which is almost realized in the two BL case. In contrast to the rather strong intrabilayer relaxation Δd_{12}, the first interbilayer relaxation Δd_{23} is very small, indicating a strong coupling between the bilayers. This is also found experimentally[12] and opposed to what we found for the Bi(111) films, where the intrabilayer coupling was strong. This trend clearly reflects the fact that in the (111) layers, all nearest-neighbor bonds can be saturated, while in the (110) layers, a dangling bond remains. Therefore, films with an even number of (110) bilayers are structurally far more stable than odd-numbered ones, a trend that was also seen for the A17 allotrope.[4] Furthermore, this difference between films with even and odd numbers of bilayers can be seen clearly in the electronic structure, as will be shown below.

2. Electronic properties

If the electronic band structure of bulk Bi is projected onto the (110) plane, the electron pockets which were located at the four L points of the rhombohedral BZ can be found in the middle of the edges of the surface Brillouin zone (SBZ) (points $\bar{X}_1$ and $\bar{X}_2$). The hole pockets, which were at the two T points in the bulk, are projected on the $\bar{X}_2$ points only, which are on the longer edges of the SBZ.[22]

In the case of the single Bi(110) bilayer (top left of Fig. 5), it is clearly visible that the p bands of Bi separate into $p_{x,y}$-type bands with a strong bonding-antibonding splitting around E_F, while the p_z bands are located at the Fermi level. The lower (occupied) p_z band crosses the Fermi level just in a small region around the $\bar{X}$ points and touches the upper p_z band at $\bar{M}$. This behavior is completely changed for the two BL case: here, also the p_z states form bonding and antibonding bands which are widely split around E_F in the vicinity of the $\bar{M}$ point and open even a tiny band gap, as can be confirmed from the density of states, Fig. 6. In contrast, the three BL film is metallic again, although with a small DOS at E_F. Again, the p_z states can be found in the wide, projected band gap around the $\bar{M}$ point, and actually they can be regarded as a precursor of the surface state band that is observed on the Bi(110) surface.[8,22] The four BL film is once more semiconducting (see also Fig. 6) with a band structure very similar to the two BL case. This even-odd pattern continues also in the thicker films. In the limit of infinite film thickness, i.e., when we consider the (110) surface of a bulk crystal, at the Fermi level, a surface state can be observed. Along the line $\overline{X_2MX_1}$, this surface state is quite similar to the states at E_F of the odd-numbered bilayers, while on the line $\overline{X_1\Gamma X_2}$, the dispersion is similar to the six BL case: a wide, Rashba-split state with holelike dispersion.[8]

In a single bilayer, the $p_{x,y}$-type states connect to a first approximation zigzag chains of Bi atoms, while the nonbonding p_z-states are directed toward the upper and lower vacuums in an alternating fashion. In a double bilayer, these p_z states bond to form a stable unit, the double bilayer. However, in a three BL film, only the middle layer can form bonds to saturate all its valences, while every second atom of the upper and lower bilayers retains a dangling bond. The four BL film can be viewed as consisting of two double bilayers, while in the five BL case, we find again a dangling bond at half of the atoms at the surfaces (cf., Fig. 7). This situation is also realized in the semi-infinite case, and indeed

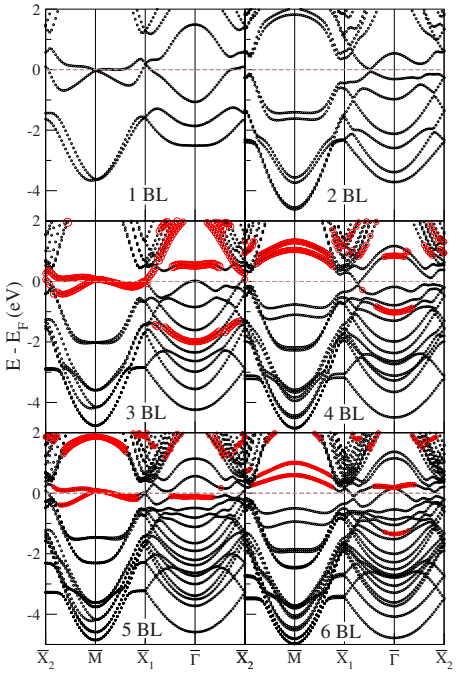

FIG. 5. (Color online) Band structures of Bi(110) films with one to six bilayer thickness. In the three to six BL band structures, states located predominantly (more than 10%) in the vacuum are marked by full (red) circles. All band structures were obtained for the relaxed geometries including spin-orbit coupling.

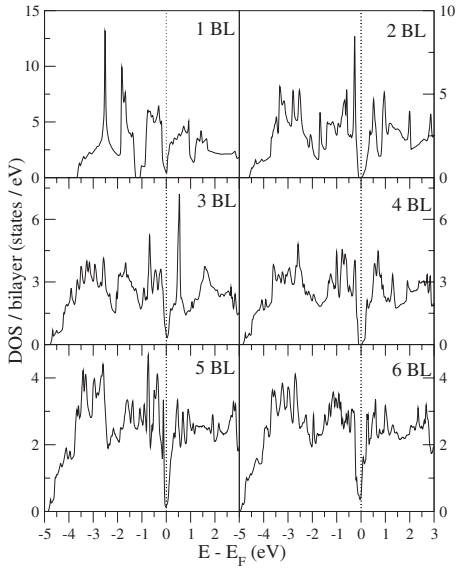

FIG. 6. Density of states for Bi(110) films of one BL to six BL thickness, normalized to the number of states of a single bilayer. The electronic structure was obtained including spin-orbit coupling.

in STM measurements, it is found that only one half of the surface atoms is visible.[8]

3. Fermi surfaces

For electronic transport which is mediated by the surface states (or precursors of surface states) described in the last paragraph, the Fermi surface is finally one of the most important quantities. As can be inferred from Fig. 8, all odd-numbered bilayers show very similar features: hole pockets around the $\bar{M}$ and $\bar{X}_2$ points and an electron pocket on the line $\overline{MX}_1$ (although the latter one is barely visible in the single BL case). These features are also present in the semi-infinite case.[8] Additionally, we can find a hole pocket around

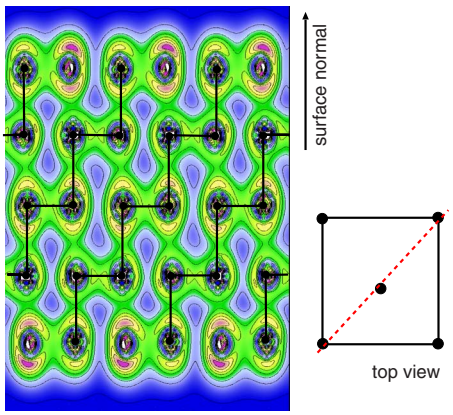

FIG. 7. (Color online) Charge density contours for the surface state (occupied bands within 0.5 eV from the Fermi level) for a five BL Bi(110) film (left). The dangling bonds can clearly be seen in red, the saturated bonds are marked with black lines. A top view of the geometry of the film and the plane, where the cut was taken, is sketched to the right.

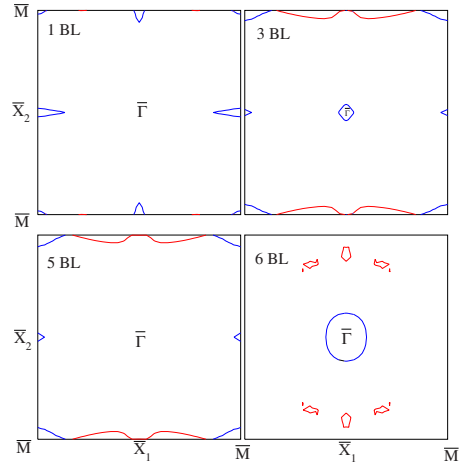

FIG. 8. (Color online) Fermi surfaces for Bi(110) films of one BL, three BL, five BL, and six BL thickness. The electronic structure was obtained including spin-orbit coupling. Electron pockets are shown in red and hole pockets in blue color.

$\bar{X}_1$ for one BL, which disappears for larger film thicknesses, and a hole pocket around $\bar{\Gamma}$ for the three BL film, which is also present at the (bulk) Bi(110) surface, although larger in this case, similar to what can be found for the six BL film. In the latter film, the pockets that are located at the Brillouin-zone boundaries in the thinner films are completely missing; instead, a small electron pocket exists on the line $\overline{\Gamma X}_1$, which is neighbored by two additional pockets in the interior of the two-dimensional Brillouin-zone.

IV. DISCUSSION AND SUMMARY

The electronic structure of thin Bi films and Bi surfaces shows a wide variety of properties, ranging from semiconducting to semimetallic or metallic behavior. The metallic states are localized at the surface, while the interior of the material lacks states, which could contribute significantly to the conductivity. A remarkable property of the metallic surface states of Bi is furthermore their Rashba-type spin-orbit splitting.[7] Spin-dependent interference processes have already been observed on the Bi(110) surface,[8] and also in thin Bi films, a spin polarization was observed experimentally.[9] Of course, in a freestanding thin Bi films, that shows inversion symmetry, no spin-polarized states can form. The states of these films which are localized equally on both sides of the film, show on the other hand a *local* spin polarization on a particular side of the film, which is compensated on the other side. As the films grow thicker, the interaction of the two surfaces of the film will decrease and at some point decouple the surface states. Likewise, a small perturbation on one side of the film (e.g., a weakly interacting substrate) will also lead to an asymmetry of the states on the two sides of the film and an effective decoupling. Therefore, it is reasonable to expect spin-polarized surface states also for thin films, although the degree of spin polarization may vary, depending on the position of the state in reciprocal space and its coupling with the bulklike states. For example, the states

along $\overline{\Gamma M}$ in a ten BL Bi(111) film (cf., Fig. 2) gradually loose their spin polarization as the $\bar{M}$ point is approached.[5,9]

We think that the strong Rashba-type splitting and the unique shapes of the Fermi surfaces will give rise to interesting conductive properties, especially as far as the spin-transport is concerned. For the honeycomblike lattice on the Bi(111) surface, it was shown in a simplified model that a variety of spin-accumulation patterns can be found, depending on the bias voltage and the direction where this voltage is applied.[23] We hope that in the future thin Bi films will provide a fruitful playground to investigate these effects both theoretically and experimentally.

ACKNOWLEDGMENTS

G.B. acknowledges the hospitality of the Donostia International Physics Center, where parts of this work originated. E.V.C. acknowledges the partial support from the University of the Basque Country (9/UPV 00206.215-13639/2001) and the Departamento de Educación del Gobierno Vasco.

[1] K. S. Novoselov, A. K. Geim, S. V. Morozov, D. Jiang, M. I. Katsnelson, I. V. Grigorieva, S. V. Dubonos, and A. A. Firsov, Nature (London) **438**, 197 (2005).
[2] C. L. Kane and E. J. Mele, Phys. Rev. Lett. **95**, 226801 (2005).
[3] S. Murakami, Phys. Rev. Lett. **97**, 236805 (2006).
[4] T. Nagao, J. T. Sadowski, M. Saito, S. Yaginuma, Y. Fujikawa, T. Kogure, T. Ohno, Y. Hasegawa, S. Hasegawa, and T. Sakurai, Phys. Rev. Lett. **93**, 105501 (2004).
[5] T. Hirahara, T. Nagao, I. Matsuda, G. Bihlmayer, E. V. Chulkov, Yu. M. Koroteev, P. M. Echenique, M. Saito, and S. Hasegawa, Phys. Rev. Lett. **97**, 146803 (2006).
[6] T. Hirahara, T. Nagao, I. Matsuda, G. Bihlmayer, E. V. Chulkov, Yu. M. Koroteev, and S. Hasegawa, Phys. Rev. B **75**, 035422 (2007).
[7] Yu. M. Koroteev, G. Bihlmayer, J. E. Gayone, E. V. Chulkov, S. Blügel, P. M. Echenique, and Ph. Hofmann, Phys. Rev. Lett. **93**, 046403 (2004).
[8] J. I. Pascual, G. Bihlmayer, Yu. M. Koroteev, H.-P. Rust, G. Ceballos, M. Hansmann, K. Horn, E. V. Chulkov, S. Blügel, P. M. Echenique, and Ph. Hofmann, Phys. Rev. Lett. **93**, 196802 (2004).
[9] T. Hirahara, K. Miyamoto, I. Matsuda, T. Kadono, A. Kimura, T. Nagao, G. Bihlmayer, E. V. Chulkov, S. Qiao, K. Shimada, H. Namatame, M. Taniguchi, and S. Hasegawa, Phys. Rev. B **76**, 153305 (2007).
[10] H. Mönig, J. Sun, Yu. M. Koroteev, G. Bihlmayer, J. Wells, E. V. Chulkov, K. Pohl, and Ph. Hofmann, Phys. Rev. B **72**, 085410 (2005).
[11] Ch. R. Ast and H. Höchst, Phys. Rev. B **67**, 113102 (2003).
[12] J. Sun, A. Mikkelsen, M. Fuglsang Jensen, Y. M. Koroteev, G. Bihlmayer, E. V. Chulkov, D. L. Adams, Ph. Hofmann, and K. Pohl, Phys. Rev. B **74**, 245406 (2006).
[13] Ph. Hofmann, J. E. Gayone, G. Bihlmayer, Yu. M. Koroteev, and E. V. Chulkov, Phys. Rev. B **71**, 195413 (2005).
[14] Ch. R. Ast and H. Höchst, Phys. Rev. Lett. **90**, 016403 (2003).
[15] V. L. Moruzzi, J. F. Janak, and A. R. Williams, *Calculated Electronic Properties of Metals* (Pergamon, New York 1978).
[16] E. Wimmer, H. Krakauer, M. Weinert, and A. J. Freeman, Phys. Rev. B **24**, 864 (1981); M. Weinert, E. Wimmer, and A. J. Freeman, *ibid.* **26**, 4571 (1982).
[17] See http://www.flapw.de for a program description.
[18] C. Li, A. J. Freeman, H. J. F. Jansen, and C. L. Fu, Phys. Rev. B **42**, 5433 (1990).
[19] P. Cucka and C. S. Barrett, Acta Crystallogr. **15**, 865 (1962).
[20] Ph. Hofmann, Prog. Surf. Sci. **81**, 191 (2006).
[21] A. B. Shick, J. B. Ketterson, D. L. Novikov, and A. J. Freeman, Phys. Rev. B **60**, 15484 (1999).
[22] S. Agergaard, Ch. Søndergaard, H. Li, M. B. Nielsen, S. V. Hoffmann, Z. Li, and Ph. Hofmann, New J. Phys. **3**, 15 (2001).
[23] Ming-Hao Liu, G. Bihlmayer, S. Blügel, and Ching-Ray Chang, Phys. Rev. B **76**, 121301(R) (2007).